

10–30-eV optical properties of GaN

C. G. Olson and D. W. Lynch

Ames Laboratory and Department of Physics, Iowa State University, Ames, Iowa 50011

A. Zehe*

Universidad Autónoma de Puebla, Departamento de Física, Puebla, Pue, Mexico

(Received 8 June 1981)

The reflectance of basal-plane epitaxial layers of GaN has been measured between 5 and 30 eV, and Kramers-Kronig analyzed to get the dielectric function and the electron-energy-loss function. The second derivative of the reflectance with respect to energy was obtained in the region of Ga 3*d* → conduction-band excitations. The latter show weak structure from transitions to Γ final states and stronger structures to final states along *U*, both split by the 0.40-eV Ga 3*d* spin-orbit splitting. The loss function exhibits two peaks, the stronger one at 19.0 eV, below the expected 23.3 eV, while the weaker one is at 23.2 eV.

I. INTRODUCTION

Gallium nitride is a large-band-gap semiconductor with the hexagonal wurtzite structure. It bears a close resemblance to the other Ga-V semiconductors, GaP, GaAs, and GaSb, which have the cubic zinc-blende structure. The distribution of nearest and next-nearest neighbors is nearly the same in the two structures, so the structure difference seems not to be very important for the electronic structure. It does, however, make a difference in the size and shape of the Brillouin zone and in the notation used to describe the symmetry of the wave functions. The correspondence between the bands in the two structures can be made, in part.^{1–3} The principal differences between the band structures in the zinc-blende and wurtzite structures are that there are fewer degeneracies in the wurtzite structure, and some different electric dipole selection rules for the optical properties, which lead to some optical anisotropy in the wurtzite-structured crystals.

Far less is known about the electronic structure of GaN than about the electronic structures of the other Ga compounds. The optical properties have been studied up to 12 eV,^{4–9} and there has been a study of the valence band and Ga 3*d* core levels by x-ray-induced photoemission.¹⁰ The energy bands have been calculated several times^{8,11,12} and the results compared extensively with optical data in one case.⁸

In the following we report on reflectance measurements ($\bar{E}I_c$) in the 5–30-eV region. The

spectrum above 20 eV is dominated by transitions from the Ga 3*d* levels to the conduction bands. Since the Ga 3*d* levels are nondispersive, the spectrum is related directly to the conduction-band density of states (and dipole matrix elements). To enhance the appearance of structures we have taken the second derivative of the reflectance spectra with respect to energy. We also have obtained the dielectric function and the characteristic electron energy loss spectrum by Kramers-Kronig analysis of our reflectance spectrum.

II. EXPERIMENTAL

The GaN samples were epitaxially grown on single-crystal sapphire substrates by pyrolytic deposition from Ga(CH₃)₂ in NH₃ (Ref. 13) or by solution growth from Ga in NH₃ and H₂.¹⁴ They were oriented with the *c* axis normal to the plane face and were from 3–5- μ m (pyrolytic) to 100- μ m (solution) thick. Measurements were made on the as-grown surface, on surfaces lightly polished with Al₂O₃, and on polished surfaces which were given a light etch in phosphoric acid at 90 °C.^{15,16} Spectra in the region of the band gap have been reported to be nonreproducible because of different strains in different samples brought about by differential thermal expansion between the GaN and the substrate. At higher photon energies we found the sample-to-sample differences that were not attributed to different amounts of scattering by surface roughness appeared as a loss in sharpness of struc-

tures in the reflectance.

The reflectances were measured using synchrotron radiation from the electron storage ring Tantalus. The reflectometer and techniques used have been described previously.¹⁷ There was no problem with inadequate spectral resolution or with long-wavelength scattered radiation or with second-order radiation. In order to enhance reflectance structures above 20 eV we measured the reflectance at 30° and 60° with *p*-polarized radiation. These data were recorded with a signal-to-noise ratio large enough to allow the second derivative of the reflectance with respect to energy to be taken without an inordinate amount of noise. The spectra were, however, smoothed before presentation. Such spectra give, in principle, a mixture of the reflectances and derivatives for $\vec{E} \parallel c$ and $\vec{E} \perp c$. However, at such photon energies for core level transitions the anisotropy is expected to be slight, but it may not be negligible at threshold.

III. RESULTS

Figure 1 shows the reflectance spectrum taken at near-normal incidence. The region below 12 eV agrees qualitatively with the spectra reported by others^{4,8,9} although some spectra⁹ show a reduced reflectance at the higher energies caused by non-specular scattering from surface roughness. There were differences in the magnitudes of the higher energy reflectance peaks in our data which correlated with the amount of surface roughness-induced non-specular scattered radiation which was detected by moving the detector out of the specularly reflected beam, but the effects of scattering were far less than those of Ref. 9. The spectrum of Fig. 1 was influenced negligibly by such scattering.

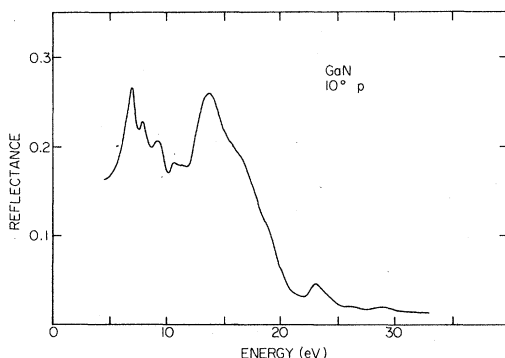


FIG. 1. Reflectance (300 K) of the basal plane at GaN single crystal taken at 10° with *p*-polarized radiation.

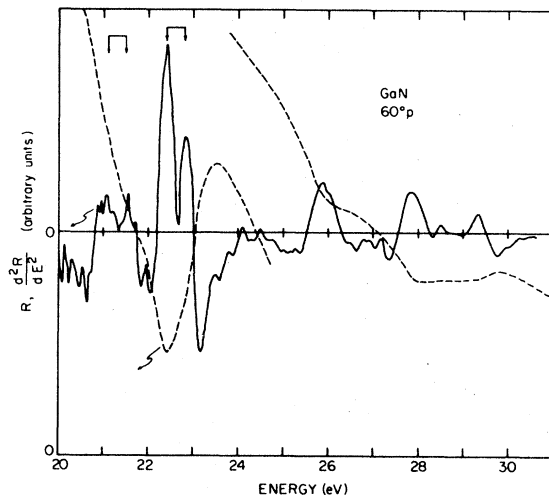


FIG. 2. Spectrum of reflected *p*-polarized phonon flux from GaN at 60° angle of incidence (dashed) and its second derivative with respect to energy. The latter is essentially d^2R/dE^2 .

A number of additional scans were made at 30° and 60° angle of incidence with *p* polarization in the region above 20 eV. Figure 2 shows this region. The spectrum of reflected light is shown by the dashed curve. This curve has not been corrected for the energy dependence of the monochromator output or the detector sensitivity. These do not contribute appreciably to the solid curve, which is the spectrum of the second derivative of the dashed curve with respect to energy. It is effectively a plot of d^2R/dE^2 for 60° *p*-polarized incident radiation.

We obtained the dielectric function $\bar{\epsilon}$ for $\vec{E} \perp c$ by a Kramers-Kronig analysis of the spectrum of Fig. 1. The extrapolation to low energy was made by using the reflectance and refractive index data in the literature.^{8,18} Above 30 eV a power-law extrapolation was used, adjusted so the falloff in reflectance with energy was parallel to that computed for GaP from the absorption coefficient in the 40–150-eV region.¹⁹ The dielectric function so obtained was similar in shape and magnitude to that previously obtained for the 2.5–10-eV region,⁸ using only data from that region, but our spectra extend to 30 eV. There is little new structure in the dielectric function, except that from the Ga 3*d* excitations, to be discussed below, and we do not display our dielectric function. The electron-energy-loss functions, however, are more interesting. They are proportional to the probability that a fast electron will lose energy *E* by exciting a longitudinal excitation in the volume and at the surface, respectively, and are $\text{Im}(-1/\bar{\epsilon})$ and $\text{Im}(-1/\bar{\epsilon}_s)$.

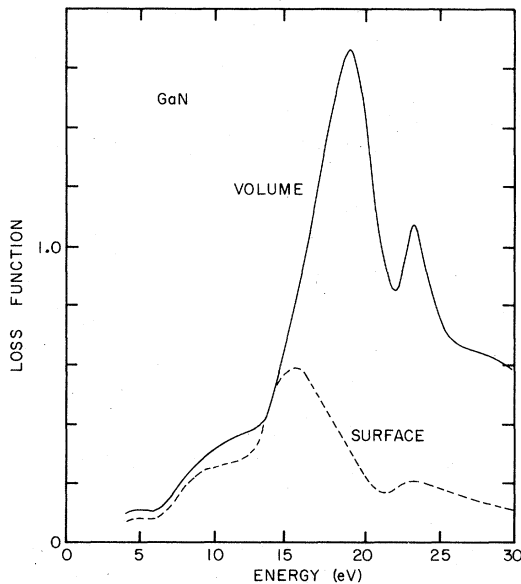


FIG. 3. Volume (solid) and surface (dashed) electron energy loss spectra of Fig. 1 by Kramers-Kronig analysis. These are $\text{Im}(-1/\tilde{\epsilon})$ and $\text{Im}[-1/(\tilde{\epsilon})]$, respectively, for $q \rightarrow 0$ and $\vec{E} \perp c$.

$[-1/(\tilde{\epsilon}+1)]$, respectively. These are shown in Fig. 3.

IV. DISCUSSION

The dielectric function can be related to the band structure via a calculation of ϵ_2 . This involves calculating electric dipole matrix elements between all possible contributing states. These are difficult to calculate, and often not very accurate. One often assumes that the matrix elements vary slowly with energy and neglects them, making the

calculated ϵ_2 proportional to the joint density of states. In the case of the excitation of Ga 3*d* electron, the initial states are just two bands, perfectly flat on the scale of our resolution, separated by the spin-orbit splitting. The contribution to ϵ_2 from either one of the spin-orbit components is then proportional to the density of states in the conduction band, with some final states not contributing if they have little Ga *p* character. Figure 4 shows the calculated energy bands for GaN and the density of states derived from them.⁸ The valence band density of states has already been compared with experiment, the x-ray photoelectron spectrum (XPS).¹⁰ The overall widths agree and the two principal peaks occur in both spectra, but the positions of the large peak at lower binding energy do not agree, having binding energies of 1.9 eV in the calculation and 3.5 eV in the XPS spectrum. The relative heights of the two peaks in the calculated spectrum are not correct either.

The conduction band density of states can be studied in the reflectance and d^2R/dE^2 spectra. The threshold for transitions can be estimated as being 21.24 eV, the sum of the binding energy of the (unresolved) Ga 3*d* levels with respect to the top of the valence band (structure *B* in Ref. 10) and the 3.5 (or 3.6) eV band gap. This quantity should be reduced by 0.16 eV to account for the threshold for the uppermost of the resolved spin-orbit split Ga 3*d* components, assuming no exciton binding energy, which may be of the order of 0.1–0.2 eV.²⁰

These transitions should exhibit the spin-orbit splitting of the Ga 3*d* levels, about 0.40 eV. Transitions from these levels should occur to any conduction-band states with a significant admix-

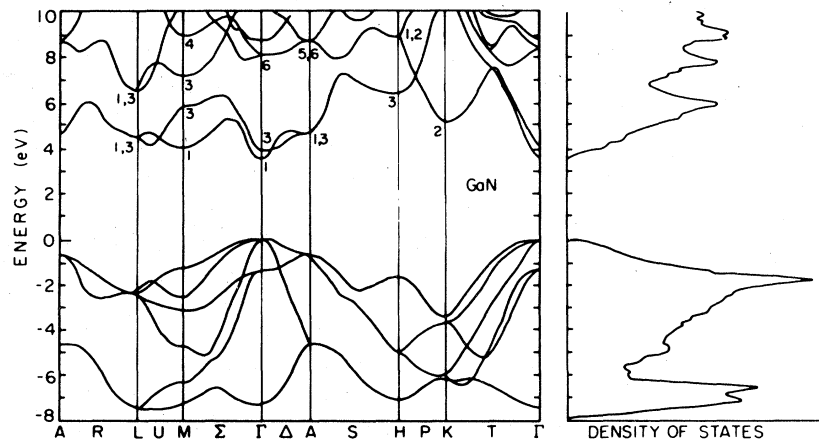


FIG. 4. Calculated band structure and density of states for GaN (from Ref. 8).

ture of p character on the Ga site. Usually those transitions to critical points in the conduction band will be emphasized in the d^2R/dE^2 spectrum, the interband critical point energies being close to the energies of the peaks in the second derivative spectra at 60° .

Maxima appear in the calculated conduction-band density of states at energies of 2.5, 4.2, and 5.2 eV above the conduction-band minimum. These maxima arise from the contributions of more than one critical point. Moreover, in the derivative spectra, weak sharp structures tend to be emphasized rather than large broad ones, so a one-to-one mapping of the density of states is not expected.

There is weak structure in the reflectance and its energy derivatives beginning about 20.5 eV, approximately where the onset of transitions from the Ga $3d$ levels is expected. These are weak signals in d^2R/dE^2 , arising from a very slight change in slope of the reflectance spectrum, but they occurred in all samples and do exhibit the expected spin-orbit splitting of the Ga $3d$ levels, 0.4 eV, as marked in Fig. 2. We believe these structures arise from transitions to the absolute conduction band minimum at Γ , a Γ_1 state with some Ga p character. The structure is weak because of a small phase space volume about Γ , but detectable because it is at threshold and there is little background, just the diminishing background of valence-band excitations.

The next structure is far more prominent and the 0.40-eV spin-orbit splitting is manifest. This doublet is 1.3-eV higher than the first structure and is four or five times stronger in the second derivative spectrum. It occurs at the energy of the minimum in the reflectance. Presumably, it represents transitions into the next lowest conduction-band minima which are allowed.

There are additional structures in Fig. 2, peaks at 25.9 and 27.8 eV. These do not show any splitting and their widths are such that there appear not to be any unresolved structures as far apart as 0.4 eV. These peaks occur 4.5 and 6.5 above the onset of transitions from the core levels to the conduction-band minimum. The lack of spin-orbit splitting probably arises because these are composite peaks from overlapping degenerate, but not equivalent, conduction-band critical points of different types, giving different line shapes.

From Fig. 4 we see that the second conduction-band minimum is the Γ_3 minimum, only 0.4 eV above the absolute Γ_1 minimum. This small

crystal-field splitting is about the same as the spin-orbit splitting of the Ga $3d$ levels. A simple calculation, based on the degeneracies of the initial and final states and assuming the 0.4-eV $\Gamma_1-\Gamma_3$ splitting is correct, shows that we expect three structures at threshold, with 0.4 eV between them, with weights of 3, 8, and 4 in order of increasing energy, neglecting matrix elements. The third component at higher energy is not apparent in the spectra, and the two components occur as in the nearly equal intensities. We note that in other wurtzite-structured semiconductors, e.g., ZnS,³ the corresponding crystal-field splitting is much larger, 1 eV and more, due to greater ionicity in the latter two compounds. If the ionicity of GaN were higher than that "assumed" in the band calculations, then the $\Gamma_1-\Gamma_3$ gap in the conduction bands would be larger, and only two structures would appear below the larger pair of structures, giving qualitative agreement of the band structure with Fig. 2. Moreover, the Γ_3 minimum probably has little Ga p character and it should not yield detectable spectral features.

About 1–1.5 eV above the Γ_1 and Γ_3 minima there are many conduction-band critical points, at points M , L , and A , and along the U line.⁸ The bands of ZnS (wurtzite structure) show a considerably larger energy difference between the conduction-band minimum and the states in the same band on the zone boundary, at M , L , and A , and along U .³ We believe a similar larger separation is appropriate for GaN as well, placing the M_1 , $L_{1,3}$, and $A_{1,3}$ points and the U_1 and U_3 lines about 1–1.5 eV above Γ_1 . It is tempting to associate the strong structure in Fig. 2 with the Ga $3d \rightarrow X_1^{cb}$ transitions which dominate the corresponding spectra of the zinc-blende-structured Ga-V compounds.^{20,21} The X points in the Brillouin zone for the zinc-blende structure map into points along the line U for the wurtzite structure, as do six of the zinc-blende L points,³ which also contribute more than do the zinc-blende Γ points to such spectra.^{21,22} The Ga $3d \rightarrow X_1$ transitions give the largest contribution to the electroreflectance spectra of GaP and GaAs in this spectral region, and transitions to L_1 points give a smaller contribution. Thus, the corresponding transitions to the minima along the U_1 lines, probably at M_1 , probably cause the large structure in d^2R/dE^2 , beginning 1.3 eV above the threshold. This raises the M_1 point about 0.2 eV above its calculated position with respect to Γ_1 , but it need not alter assignments of interband optical transitions given by Bloom *et al.*⁸

The electron-energy-loss function, Fig. 3, is interesting in that it displays two peaks, each representing a longitudinal volume excitation. The free electron plasmon energy $\hbar\omega_p$ is 22.04 eV while the expected value of the plasmon in a system with a band gap of E_g is $[(\hbar\omega)^2 + E_g^2]^{1/2} = 23.3$ eV. The principal loss function peak is at 19.0 eV and the secondary peak is at 23.2 eV. ϵ_1 passes through zero at 17.2 eV, so the occurrence of the double peak and the shift of the lower one from the free-electron value is influenced by the interband and Ga 3d core-level transitions. In fact, the minimum between the peaks is at 22 eV, about the onset of the stronger transitions from the Ga 3d levels. The double structure in the loss function can also be seen in the XPS spectrum of the Ga 3d levels as a pair of satellite peaks (Ref. 10, Fig. 1). The loss functions of GaN, GaAs, and GaSb do not show such prominent "second" loss-function

peaks at higher energies, showing instead a weak doublet probably arising directly from the Ga 3d excitations.²³

ACKNOWLEDGMENTS

We wish to thank W. H. Petzke, Sektion Chemie, Universität Leipzig, and R. A. Logan, Bell Laboratories, for several samples of GaN. The Ames Laboratory is operated for the U.S. Department of Energy by Iowa State University under Contract No. W-7405-Eng-82. This research was supported in part by the Director for Energy Research, Office of Basic Energy Sciences, Contract No. WPAS-KC-02-02-02. The storage ring is operated by the Synchrotron Radiation Center, University of Wisconsin-Madison, under Contract No. DMR 7721888 National Science Foundation.

*Present address: Sektion Physik, Technische Universität Dresden, Mommenstrasse 13, 8027 Dresden, German Democratic Republic.

¹J. L. Birman, Phys. Rev. **115**, 1493 (1959).

²M. Cardona and G. Harbeke, Phys. Rev. **137**, A1467 (1965).

³T. K. Bergstresser and M. L. Cohen, Phys. Rev. **164**, 1069 (1967).

⁴B. B. Kosicki, R. J. Powell, and J. C. Burgiel, Phys. Rev. Lett. **24**, 1421 (1970).

⁵R. Dingle, D. D. Sell, S. E. Stokowski, P. J. Dean, and R. B. Zetterstrom, Phys. Rev. B **3**, 497 (1971).

⁶R. Dingle, D. D. Sell, S. E. Stokowski, and M. Hegems, Phys. Rev. B **4**, 1211 (1971).

⁷B. Monemar, Phys. Rev. B **10**, 676 (1974).

⁸S. Bloom, G. Harbeke, E. Meier, and I. B. Ortenburger, Phys. Status Solidi B **66**, 161 (1974).

⁹V. V. Sobolev, S. G. Kroitoru, E. B. Sokolov, and V. P. Chegnov, Fiz. Tverd. Tela (Leningrad) **20**, 3743 (1978) [Sov. Phys. — Solid State **20**, 2167 (1978)].

¹⁰J. Hedman and N. Mårtensson, Phys. Scr. **22**, 176 (1980).

¹¹D. Jones and A. H. Lettington, Solid State Commun. **11**, 701 (1972).

¹²J. Bourne and R. L. Jacobs, J. Phys. C **5**, 3462 (1972).

¹³W. -H. Petzke and A. Zehe, Krist. Tech. **10**, 135

(1975).

¹⁴R. A. Logan and C. D. Thurmond, J. Electrochem. Soc. **119**, 1726 (1972).

¹⁵Y. Morimoto, J. Electrochem. Soc. **121**, 1382 (1974).

¹⁶A. Shintari and S. Minagawa, J. Electrochem. Soc. **123**, 706 (1976).

¹⁷C. G. Olson and D. W. Lynch, Phys. Rev. B **9**, 3159 (1974).

¹⁸E. Ejder, Phys. Status Solidi A **6**, 445 (1971).

¹⁹M. Cardona, W. Gudat, B. Sonntag, and P. Y. Yu, in *Proceedings of the Tenth International Conference on the Physics of Semiconductors, Cambridge, Massachusetts, 1970*, edited by S. P. Keller, J. C. Hensel, and F. Stern (Atomic Energy Commission, Virginia, 1970).

²⁰D. E. Aspnes, C. G. Olson, and D. W. Lynch, in *Proceedings of the XIII International Conference of the Physics of Semiconductors, Rome, 1976*, edited by F. G. Fumi (Tipografia Marves, Rome, 1976), p. 1000.

²¹D. E. Aspnes, C. G. Olson, and D. W. Lynch, Phys. Rev. B **12**, 2527 (1975).

²²D. E. Aspnes, C. G. Olson, and D. W. Lynch, Phys. Rev. Lett. **37**, 766 (1976).

²³C. V. Festenberg, Z. Phys. **227**, 453 (1969).